

Theory of Infrared and Raman Spectra of Amorphous Si and Ge†

R. Alben

Department of Engineering and Applied Science, Yale University, New Haven, Connecticut 06520

and

J. E. Smith, Jr., and M. H. Brodsky

IBM Thomas J. Watson Research Center, Yorktown Heights, New York 10598

and

D. Weaire

Department of Engineering and Applied Science, Yale University, New Haven, Connecticut 06520

(Received 20 February 1973)

A theory of infrared and Raman spectra, based on a two-parameter elastic energy and simple local-bond optical coupling mechanisms, is developed for amorphous silicon (*a*-Si) and amorphous germanium (*a*-Ge). When the theory is applied to a random-network structural model the results are in satisfactory agreement with experiment, especially with regard to the qualitative differences between the infrared and Raman spectra. Results for simple microcrystalline models are also presented.

In amorphous materials the absence of long-range order implies that all vibrational modes are to some degree both infrared and Raman active. The infrared and Raman spectra should therefore resemble the vibrational density of states, with modifications due to the matrix elements which determine the relative strengths of the contributions of different modes to the spectra. Experimental measurements^{1,2} of infrared and Raman spectra of *a*-Si and *a*-Ge seem to reflect a density of states like that of their crystalline counterparts, but modified by smoothly varying matrix elements. In a recent Letter,³ the general form of this density of states was explained by a theorem applicable to all tetrahedrally bonded structures. In this Letter, we present a theory for the infrared and Raman spectra including matrix element effects. Our results for a representation of the continuous random-network (CRN) model agree quite well with experiment. On the other hand, we are unable to obtain such agreement with strain-free diamond or wurtzite microcrystalline models. More complicated microcrystalline models based on crystal structures with larger unit cells, or incorporating internal strains, are not considered here. Fuller details of the calculation and results for a larger set of plausible structural models will be the subject of a future publication.

Our procedure is to perform numerical calculations for the normal modes and spectra of tetrahedrally coordinated clusters of from 55 to 64 atoms with a simple two-parameter elastic

energy⁴ and simple bond mechanisms for the coupling of light and atomic displacements. For infrared activity, we assume a displacement-dependent dipole moment \vec{M} of the form:

$$\vec{M} = \sum_{l\{\Delta,\Delta'\}} \{\vec{r}_{\Delta'}(l) - \vec{r}_{\Delta}(l)\} \times \{[\vec{u}_l - \vec{u}_{l\Delta}] \cdot \vec{r}_{\Delta}(l) - [\vec{u}_l - \vec{u}_{l\Delta'}] \cdot \vec{r}_{\Delta'}(l)\}, \quad (1)$$

where the sum is over all atoms l and distinct pairs of neighbors specified by Δ and Δ' ; the displacements are given by \vec{u}_l , and $\vec{r}_{\Delta}(l)$ is the unit vector from the equilibrium position of atom l to its neighbor $l\Delta$. This mechanism, involving triads of atoms, is of the simplest type which can be employed for a homopolar material⁵ and represents displacements of negative charge from extended to compressed bonds.

For Raman activity we consider the following forms as contributions to the displacement-dependent polarizability:

$$\vec{\alpha}_1 = \sum_{l\Delta} [\vec{r}_{\Delta}(l) \vec{r}_{\Delta}(l) - \frac{1}{3} \vec{I}] \vec{u}_l \cdot \vec{r}_{\Delta}(l), \quad (2a)$$

$$\vec{\alpha}_2 = \sum_{l\Delta} \left\{ \frac{1}{2} [\vec{r}_{\Delta}(l) \vec{u}_l + \vec{u}_l \vec{r}_{\Delta}(l)] - \frac{1}{3} \vec{I} \vec{u}_l \cdot \vec{r}_{\Delta}(l) \right\}, \quad (2b)$$

$$\vec{\alpha}_3 = \sum_{l\Delta} \vec{I} \vec{u}_l \cdot \vec{r}_{\Delta}(l), \quad (2c)$$

where \vec{I} is the unit dyadic. If the Raman tensor is approximated by a sum of contributions from every pair of nearest neighbors, i.e., every bond, and each of these contributions is invariant under rotations about the bond, it is given by a combination of 2(a)-2(c). The first and sec-

ond mechanisms describe the changes in the anisotropic part of the polarizability with bond length and bond direction, respectively, and the third mechanism describes the displacement-induced change in the isotropic part of the polarizability. The first mechanism gives rise to Raman scattering in diamond, wurtzite, and other perfectly tetrahedrally bonded structures as well as in distorted structures, while the second and third mechanisms only contribute to the extent that there are distortions from perfect tetrahedral bonding. Local-bond concepts have proved useful in understanding many semiconductor properties for which a first-principles treatment is prohibitively difficult.⁶ Thus the local-bond mechanisms of Eqs. (1) and (2) should be regarded as first approximations which should provide an understanding of the major features of the spectra.⁷ Of course, for crys-

talline structures they result in nonzero activity only for those modes which have correct symmetries—a fact which provides a convenient check in such calculations.

In Fig. 1(a), we show the experimental infrared² and reduced^{1,8} Raman spectra of α -Si. (Results for α -Ge are quite similar.^{1,2}) Only the HH⁹ Raman spectrum is shown since the HV⁹ spectrum was similar in shape. We have measured the depolarization ratio (HV/HH) at the peak of the Raman spectrum and found it to be 0.8 ± 0.1 , which indicates that the depolarization is quite close to 0.75, the theoretical maximum for a macroscopically isotropic sample.

In Fig. 1(b), we show the results of calculations for the density of states and infrared and Raman spectra for a 61-atom periodic CRN model with force constants appropriate to crystalline Si. The model was handbuilt by D. Hender-

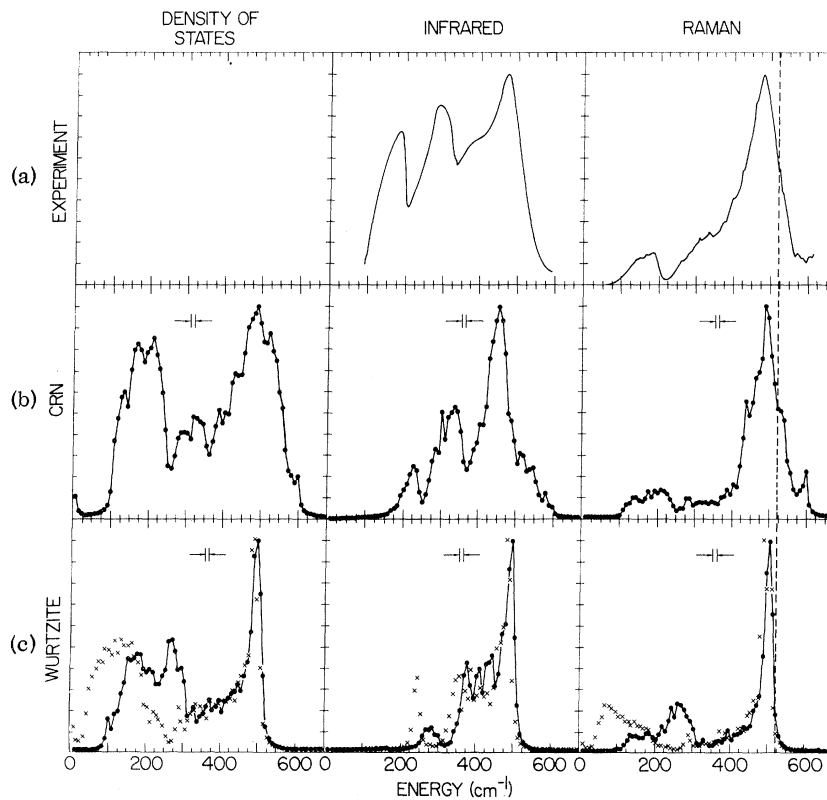


FIG. 1. Experimental and calculated spectra for amorphous Si. Vibrational densities of states, infrared absorption constants, and reduced Raman spectra are given. (The HV Raman spectra have the same shape as HH, so only HH is shown.) The spectra in the top row are experimental results from Refs. 1 and 2; center row, calculations for a 61-atom representation of a continuous random network; bottom row, calculations for a 64-atom wurtzite-structure crystallite with fixed (connected points) and free (crosses) boundary conditions. The calculated spectra were constructed by adding Lorentzians from each of the modes, and sampling the resulting distribution at the plotted points. Note the width of the Lorentzians used in this smoothing procedure (indicated by vertical bars), which is smaller than the width of the various peaks in the spectra. The dashed line in the Raman spectra indicates the energy of the Raman line in diamond-structure Si. All spectra were normalized to the same height.

son¹⁰ and refined by a numerical procedure. It may be regarded as a crystal with a large unit cell and a Brillouin zone which is so small that the 183 zone center modes should adequately represent the character of the modes of an extended CRN structure. In the calculation of the infrared spectrum there were no adjustable parameters apart from the normalization. For the Raman spectrum, there were two adjustable parameters [the relative weighting of 2(a)-2(c)] in addition to normalization. It was found that best agreement with experiment was obtained with a displacement-dependent polarizability proportional to $\alpha_1 + 3\alpha_2$. The choice of zero for the coefficient of the α_3 term is necessary if the calculation is to be in accord with the observed similarity of HH and HV spectra and the observed depolarization ratio.

The overall agreement between the calculated spectra for the CRN model and the experiments is reasonably good. The relative weights of the lower, middle, and upper parts of the observed spectra are reproduced rather well by the calculations and it is particularly satisfactory that the difference in these relative weights in the infrared and Raman spectra is reproduced. This difference can be explained in terms of the qualitative nature of the vibrational modes in the various parts of the spectrum.³ We feel that, with due allowance for the simplicity of the theory which we have used, the results based on the use of the random network model are entirely satisfactory.

Rudee and Howie have suggested,¹¹ on the basis of dark-field electron-microscopy studies, that *a*-Ge and *a*-Si contain a substantial fraction of wurtzite crystallites containing about 100-150 atoms. With this suggestion in mind, we have performed calculations on a structure representing a microcrystallite of wurtzite Si with fixed and free boundary conditions. The results from our model, in which more than 60% of the 64 atoms have at least one "boundary bond," should enable us to examine an upper limit for the effects of grain boundaries on the spectra for the proposed structure. In our calculation with fixed boundary conditions, modeled by distorted bonding to fixed atoms outside the cluster, and free boundary conditions, represented by broken boundary bonds, infrared and Raman activity occurs in all modes.

In Fig. 1(c), we show infrared and Raman spectra for both fixed and free boundary conditions and the same mechanisms as used in the CRN

model. Contributions from boundary bonds were excluded from the calculation of the infrared spectrum since they were found to make a large contribution which worsened agreement with experiment. The calculated spectrum remained quite sensitive to boundary conditions, as might be expected, since infrared activity would vanish for an infinite wurtzite crystal. This makes it difficult to make inferences regarding the validity of the microcrystallite model on the basis of the infrared spectrum. We therefore attach more significance to the calculated Raman spectrum, particularly the sharpness of the upper peak, which is quite insensitive to boundary conditions and the free parameters in the calculations. The broadening of the peak seen in the experiments thus cannot be solely due to boundary effects on wurtzite microcrystallites of the size proposed by Rudee and Howie. It seems that it would be necessary to construct more complicated microcrystalline models, with large internal strain-broadening mechanisms or based on crystals with larger unit cells, to obtain as good agreement with experiment as was achieved in the straightforward CRN calculation which we have presented.

We would like to acknowledge several helpful discussions with G. S. Cargill, III, W. Cochran, and S. C. Moss. Thanks are again due to D. Henderson for supplying us with the coordinates of his random-network model.

†Work supported in part by the U. S. Air Force Office of Scientific Research under Contract No. F44620-71-C-0039 and by the National Science Foundation under Contract No. GH-35999.

¹J. E. Smith, Jr., M. H. Brodsky, B. L. Crowder, M. I. Nathan, and A. Pinczuk, *Phys. Rev. Lett.* **26**, 642 (1971); J. E. Smith, Jr., M. H. Brodsky, B. L. Crowder, and M. I. Nathan, in *Proceedings of the Second International Conference on Light Scattering in Solids*, edited by M. Balkanski (Flammarion, Paris, 1971), p. 330.

²A. Lurio and M. H. Brodsky, *Bull. Amer. Phys. Soc.* **17**, 322 (1972), and further unpublished results.

³D. Weaire and R. Alben, *Phys. Rev. Lett.* **29**, 1505 (1972).

⁴P. N. Keating, *Phys. Rev.* **145**, 637 (1966). We have used $\alpha = 0.475 \times 10^5$ dyn/cm and $\beta/\alpha = 0.2$. These are the same values as those used in a previous study of Si III and Ge III [R. J. Kobliska, S. A. Solin, M. Selders, R. K. Chang, R. Alben, M. F. Thorpe, and D. Weaire, *Phys. Rev. Lett.* **29**, 725 (1972)]. The precise choice of β/α is somewhat arbitrary—a small change would not affect our conclusions.

⁵I. Chen and R. Zallen, Phys. Rev. 173, 833 (1968).

⁶J. C. Phillips, *Covalent Bonding in Crystals, Molecules and Polymers* (Univ. of Chicago Press, Chicago, Ill., 1966).

⁷Kobliska *et al.*, Ref. 4.

⁸R. Shuker and R. W. Gammon, Phys. Rev. Lett. 25, 222 (1970).

⁹HH and HV denote the relative polarizations of the exciting and analyzed light. HH refers to the configuration where both are horizontal, and HV to that for which one is horizontal and the other vertical.

¹⁰D. Henderson, private communication.

¹¹M. L. Rudee and A. Howie, Phil. Mag. 25, 1001 (1972); M. L. Rudee, Thin Solid Films 12, 207 (1972).

Observation of Giant Kohn Anomaly in the One-Dimensional Conductor $K_2Pt(CN)_4Br_{0.3} \cdot 3H_2O$

B. Renker, H. Rietschel, L. Pintschovius, and W. Gläser

Institut für Angewandte Kernphysik, Kernforschungszentrum Karlsruhe, 75 Karlsruhe, Germany

and

P. Brüesch, D. Kuse, and M. J. Rice

Brown Boveri Research Center, CH-5401 Baden, Switzerland

(Received 19 March 1973)

Longitudinal acoustic phonons have been measured by coherent inelastic neutron scattering in the direction of the platinum chains of a single crystal of the one-dimensional conductor $K_2Pt(CN)_4Br_{0.3} \cdot 3H_2O$ at room temperature. The phonon dispersion curve shows a pronounced anomaly at the phonon wave number $q_0 = 0.32 \text{ \AA}^{-1}$ and is interpreted as the logarithmic Kohn anomaly characteristic of a one-dimensional metal.

The properties of the "mixed-valence" square planar compounds of platinum such as $K_2Pt(CN)_4Br_{0.3} \cdot 3H_2O$ have been of much interest recently because of their almost one-dimensional (1D) conductivity.¹ A detailed analysis of the structure of this and related compounds has been reported by Krogmann and Hausen.² In $K_2Pt(CN)_5Br_{0.3} \cdot 3H_2O$ the planar $Pt(CN)_4$ complexes are stacked in such a way that the Pt atoms form linear chains with a lattice constant of 2.89 \AA . The spacing between adjacent chains is 9.87 \AA , and the crystal structure is tetragonal. It is believed that partial oxidation of the Pt ions by Br leads to a $5d_{z^2}$ conduction band which is partially empty. Kuse and Zeller³ measured the optical reflectivity of $K_2Pt(CN)_4Br_{0.3} \cdot 3H_2O$ for light polarized parallel and perpendicular to the chains, and for the former polarization observed a striking metalliclike reflectivity for photon energies below about 2 eV. On the other hand, the dc conductivity was observed to become thermally activated below 200°K , and at 4.2°K the material is an excellent insulator.¹ Several models have been proposed to explain the transition from a high-temperature conducting to a low-temperature insulating state. The interrupted-strand model^{3,4} treats the compound as consisting of metallic strands interrupted by defects. Bloch, Weisman, and Varma⁵ emphasize the singular ef-

fect of random potentials in one-dimensional systems. Both models are superseded to some extent by the recent observation of Comès *et al.*⁶ of a superstructure in the Pt strands with a period of $6c$ ($c = \text{Pt-Pt distance}$). A superstructure of this period is indeed expected to result from either a Peierls instability⁷ (static distortion) or a giant Kohn anomaly⁸ (dynamic distortion), both of which are effects peculiar to a linear chain with a partly filled conduction band. From the x-ray diffuse-scattering experiments of Comès *et al.* it was not possible to decide whether the observed superstructure is static or dynamic. Both the Peierls distortion and the Kohn anomaly result from the same driving force, the instability of the electronic kinetic energy in a one-dimensional system, and occur at a wave vector \vec{q} which is related to the Fermi wave vector k_F by $|\vec{q} + \vec{\tau}| = 2k_F$, where $\vec{\tau}$ is a reciprocal-lattice vector.

Electrical-conductivity,¹ thermopower⁹ and, in particular, ¹⁹⁵Pt nuclear-magnetic-resonance¹⁰ measurements indicate that below 100°K the compound is a band semiconductor caused by a static Peierls distortion. This view is further supported by the observation of a phase transition from a strictly one-dimensional superstructure at room temperature to a three-dimensionally ordered state at lower temperature.¹¹ If the room-